Supplementary information

Confocal rescan structured illumination microscopy for real-time deep tissue imaging with super-resolution

Shuhao Shen[a,c], E Du[a,d], Miao Zhang[a], Yuting Wen[a], Kai Long[a], Anqi Qiu[a,b] & Nanguang Chen[a,b,*]

[a] Department of Biomedical Engineering, National University of Singapore, 7 Engineering Drive 1, Singapore 117574, Singapore
[b]NUS (Suzhou) Research Institute, No. 377 Linquan Street, Suzhou Industrial Park, Suzhou, Jiangsu 215123, P. R. China
[c]Guangzhou Institute of Technology, Xidian University, Sino-Singapore Guangzhou Knowledge City，Huangpu District, Guangzhou, Guangdong 510555, P. R. China
[d]School of Microelectronics, Shenzhen Institute of Information Technology, No. 2188, Longxiang Avenue, Longgang District, Shenzhen, Guangdong 518172, P. R. China.
[*]Address all correspondence to Nanguang Chen, biecng@nus.edu.sg

List of supplementary information

NOTE S1. Principle of one-dimensional image re-scan (Page 2)

NOTE S2. Spatial resolution enhancement characterized by fluorescent beads (Page 5)

NOTE S3. Details of the CR-SIM imaging system (Page 6)

NOTE S4. Sample preparation (Page 7)

NOTE S1. Principle of one-dimensional image re-scan

To intuitively illustrate the image re-scan principle in one dimension, we describe the point spread function formation with a simplified optical system in Figure S1.

The imaging system can be modeled by two 4f systems with the sample plane (x_1), intermediate slit plane (x_2), and detection plane (x_3). For simplicity, all the optical magnifications are assumed to be 1. We also define diffraction-limited field point spread functions used for fluorescence excitation and emission as $h_{ex}(x)$ and $h_{em}(x)$. The field point spread function can be calculated using the debye integral in the case of a cylindrical lens

$$h(v) = \int_{pupil}^{d} P(\xi) \exp(-iv\xi)\, d\xi, \tag{S1}$$

where $P(\xi)$ is the pupil function and the coordinate ξ is the transverse displacement in the pupil plane, normalized by the pupil size from -1 to 1. v is the optical coordinates given by $v = 2\pi NA \cdot x/\lambda$.

To obtain the system point spread function, we position a fluorescent point object at the origin of the sample plane, which can be expressed as $\delta(x_1)$. When the illumination line focus is scanned to an offset distance *s* from the origin, the excitation field point spread function at the sample plane is simply $h_{ex}(x_1 + s)$. Without loss of generality, the fluorescence quantum yield is assumed to be 1. Therefore, the emission field from the object is given by

$$E_1(x_1, s) = |h_{ex}(x_1 + s)|\delta(x_1). \tag{S2}$$

The emission field is de-scanned by the first scanner (GM1) and propagates to the slit plane. Its distribution can be represented by $|h_{ex}(s)|h_{em}(x_2 - s)$, which has its center shifted by *s* from the origin.

A slit can be placed at the slit plane as a spatial filter. For a finite size slit, its aperture can be modeled by a piecewise function

$$D(x_2) = \begin{cases} 1, & |x_2| \le d \\ 0, & |x_2| > d \end{cases}, \tag{S3}$$

where $2d$ is the slit width. The emission field passing through the slit is simply

$$E_2(x_2, s) = |h_{ex}(s)|h_{em}(x_2 - s)D(x_2). \tag{S4}$$

This emission intensity is then rescanned by the second scanner (GM2) and mapped to the detection plane. Its distribution is also determined by h_{em} and but shifted by s', an offset depending on the angular amplitude of GM2 which may be different from that of GM1. Here we define a sweep factor (rescan ratio) η so that $s' = \eta s$. Consequently, the instantaneous field distribution in the detection plane is given by

$$\begin{aligned} E_3(x_3, s) &= \int dx_2 E_2(x_2) h_{em}(x_3 + x_2 - s') \\ &= \int dx_2 |h_{ex}(s)| h_{em}(x_3 + x_2 - s') h_{em}(x_2 - s) D(x_2) \end{aligned} \tag{S5}$$

The intensity point spread function at the detection plane can be obtained by the integration over *s*

$$\begin{aligned} I_3(x_3) &= \int ds |E_3(x_3, s)|^2 \\ &= \int ds |h_{ex}(s)|^2 \left| \int dx_2 h_{em}(x_3 + x_2 - s') h_{em}(x_2 - s) D(x_2) \right|^2 \end{aligned} \tag{S6}$$

Let's consider two extreme cases. In case an infinitely small slit is used, the slit functi1on can be represented by a delta function $\delta(x_2)$, and equation (6) can be simplified as

$$\begin{aligned} I_3(x_3) &= \int ds|h_{ex}(s)|^2|h_{em}(s)|^2|h_{em}(x_3-\eta s)|^2 \\ &= \tfrac{1}{\eta} PSF_c(x_3/\eta) \otimes PSF_w(x_3), \end{aligned} \tag{S7}$$

where $\otimes$ denotes the convolution operation. PSF_c and PSF_w are diffraction limited confocal point spread function and wide-field point spread function, respectively.

If no slit is used, the slit function becomes a constant ($D(x_2) = 1$). Then we define $s'' = (\eta - 1)s$ so that equation (6) can be rewritten as

$$\begin{aligned} I_3(x_3) &= \int |h_{ex}(s)|^2|h_{em}(x_3-(\eta-1)s)|^2 ds \\ &= \tfrac{1}{\eta-1}\int \left|h_{ex}\left(\tfrac{s''}{\eta-1}\right)\right|^2 |h_{em}(x_3-s'')|^2 ds'' \\ &= \left|h_{ex}\left(\tfrac{x_3}{\eta-1}\right)\right|^2 \otimes |h_{em}(x_3)|^2 \end{aligned} \tag{S8}$$

This detection plane PSF can be mapped back to the sample plane and it becomes

$$I_1(x_1) = \left|h_{ex}\left(\tfrac{\eta}{\eta-1}x_1\right)\right|^2 \otimes |h_{em}(\eta x_1)|^2 \tag{S9}$$

When η = 1, the system works in the normal scan mode where the intensity point spread function is reduced to $|h_{em}(x_1)|^2$, which is equivalent to PSF_w. In the case of $\eta > 1$, the system PSF is the convolution of two wide-field PSFs, which are compressed by factors of $\frac{\eta}{\eta-1}$ and η, respectively. The best scenario is $\eta = 2$ when both wide-field PSFs are squeezed equally by two times. Compared to PSF_w, the FWHM (full width at half maximum) of $I_1(x_1)$ is improved by a factor of about 1.5 in this case.

We have further numerically investigated the system behavior when the slit size is finite and the rescan ratio remains at $\eta = 2$. Shown in Fig. S2(a) are PSFs computed with Eq. 7 and different slit sizes. The coordinates x_1 is normalized to $r_0 = 0.61\,\lambda/NA$. The PSF_w is also plotted in the same figure for comparison. The PSF FWHM of the image rescan system is reduced by factors of 1.17, 1.25, 1.37, and 1.49, respectively, for slit sizes of $d = 0.1r_0, 0.5r_0, r_0, and\ 5r_0$. The slit size of $d = 5r_0$ results in a resolution enhancement very close to the open slit case, while $d = r_0$ seems a good compromise between super-resolution and background rejection. The corresponding magnitude optical transfer functions (OTFs) are provided in Fig. S2(b). The OTF of a wide-field system stops at the cut-off spatial frequency $f_c = 1/r_0$. In contrast, the spatial frequency band is stretched to $2f_c$ when $d = 5r_0$. It implies that the resolution can be enhanced by a factor of 2 instead of 1.5 if a suitable deconvolution process is followed to reshape the spectrum. For a slit size more relevant to optical sectioning (e.g., $d = r_0$), a resolution enhancement beyond 1.6 can be readily achieved with the assistance of deconvolution.

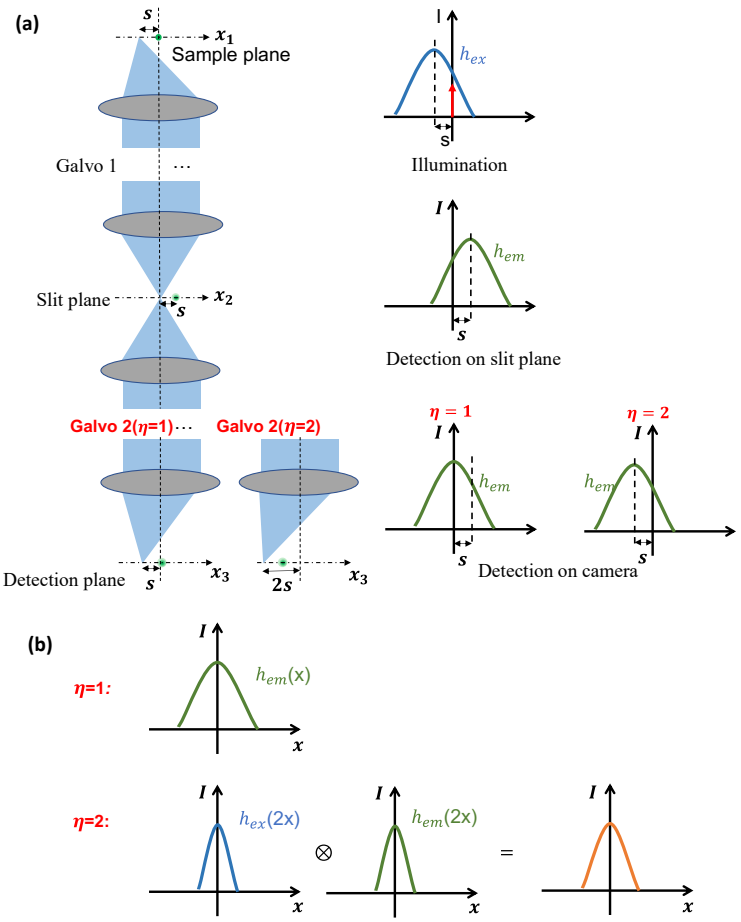

Fig. S1. (a) The image formation of a point object with normal scan ($\eta = 1$) and image rescan ($\eta = 2$). The optical diagram (left) shows the light path of the imaging process in the case that the line focus is scanned to an offset of s from the origin. The illumination and detection intensity profiles at each plane are plotted on the righthand side. (b) Comparison of system point spread function: the width of the PSF profile for the case of image rescan ($\eta = 2$) is reduced by a factor of 1.5 compared with that of a normal scan ($\eta = 1$).

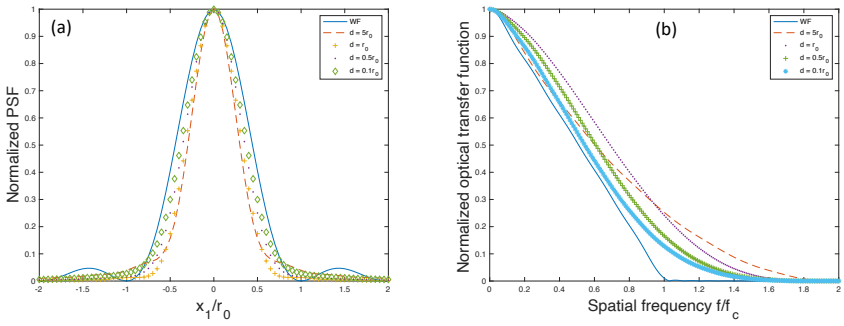

Fig. S2. Simulated resolution enhancement. (a) Point spread functions. (b) Optical transfer functions. WF: wide-field.

NOTE S2. Spatial resolution enhancement characterized by fluorescent beads

We characterized the lateral resolution of the CR-SIM system using 100 nm fluorescent beads, for which the emission filter was a bandpass (20 nm bandwidth) filter centered at 520 nm. To verify the high-resolution performance, we used a water-immersion objective lens with a high numerical aperture (NA) of 1.2 and a high magnification of 60X (UPlanSApo 60X/1.20W, Olympus) for the imaging experiment. Shown in Figure S3(a) is an LSCM image of two fluorescence beads in the focal plane. The same sample was later scanned with the CR-SIM system, and the result is shown in Figure S3(b). The CR-SIM image was further processed using Richardson-Lucy deconvolution with 10 iterations, which is shown in Figure S3(c). This deconvolution parameter was selected to achieve the highest resolution improvement and at the same time avoid overamplification of the noise that leads to the ringing artifacts. Intensity profiles along vertical and horizontal lines through the bead center were compared in Figure S3(d). Spatial resolutions measured from LSCM beads images were 291 nm in the horizontal direction and 294 nm in the vertical direction. In contrast, the CR-SIM image resolutions were 175 nm and 179 nm, respectively, in horizontal and vertical directions. The resolution improvement was 1.64-1.66X over LSCM and 1.47-1.51X over the diffraction limit. After deconvolution, the resolution improvement was 1.93-1.99X over the diffraction limit, which is nearly double the resolution band limit.

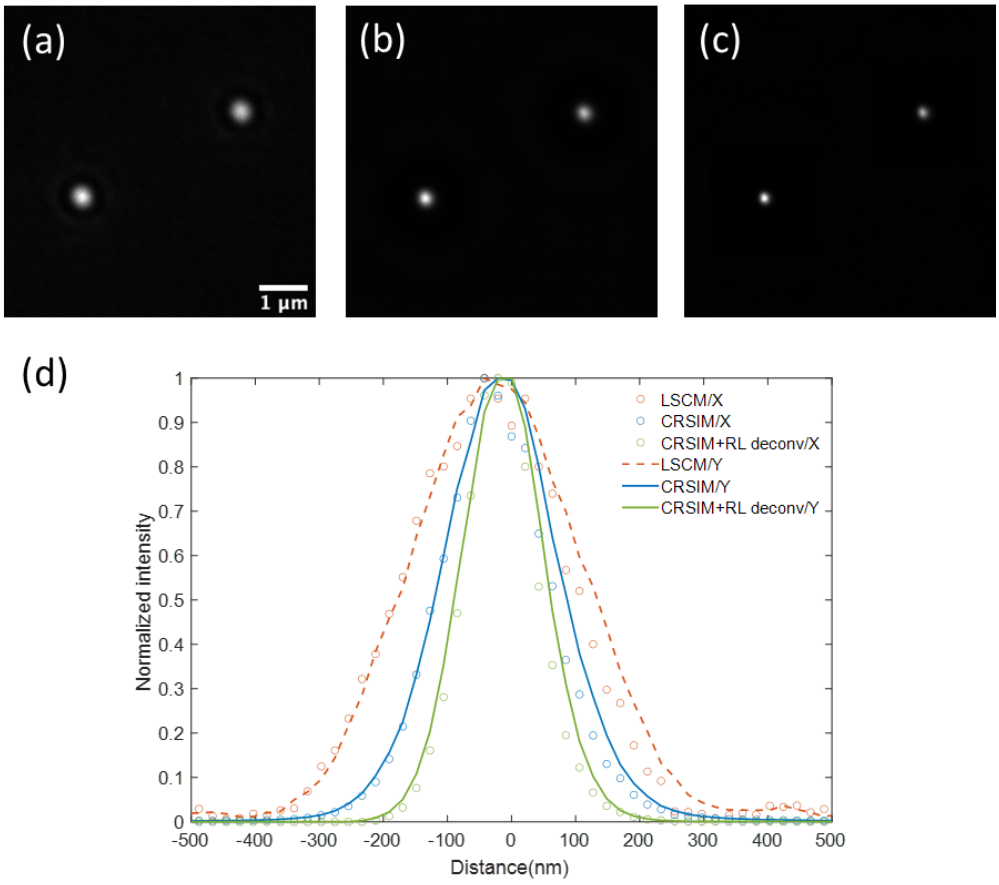

Fig. S3. (a) LSCM image, (b)CR-SIM image, and (c)CR-SIM image with Richardson-Lucy deconvolution of 100 nm fluorescent beads; (d) Intensity profiles along the vertical (Y) and horizontal (X) lines through the center of the bead at the bottom left corner of each image.

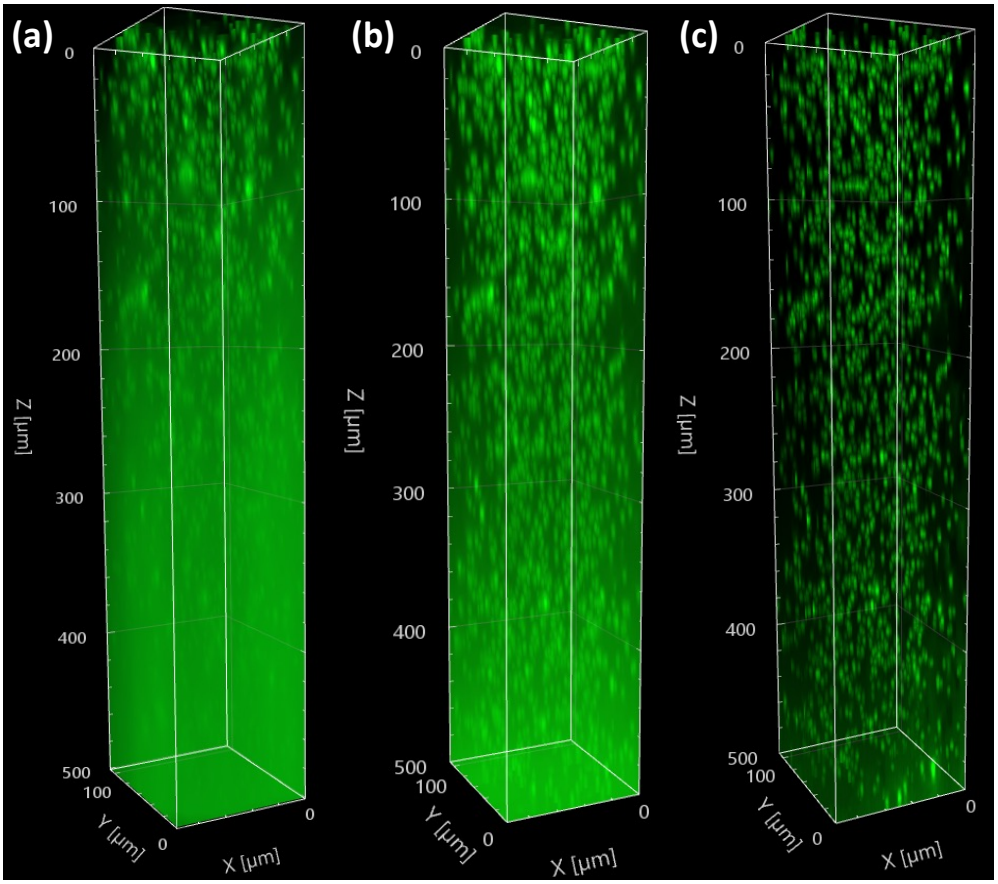

Fig. S4. 3D fluorescence intensity distribution of thick beads phantom imaged by WF-SIM(**a**), LSCM(**b**), and CR-SIM(**c**) after IMARIS volumetric rendering: depth range from 0 to 500 μm

NOTE S3. Details of the CR-SIM imaging system

The CR-SIM system includes a dual-wavelength laser (473nm/561nm, power<50mW, Cobolt) for fluorescence excitation. As in most line scan systems, a cylindrical lens (CL) creates a line focus on the sample. To achieve intensity modulation along with the line focus, a Wollaston prism (MW2S-10-5, Karl Lambrecht Corporation), used as a polarization beam splitter, angularly separates the excitation beam into two half beams. The interference between the half beams gives rise to a modulated pattern on the focal plane. In the current setup, the separation angle of the Wollaston prism is 5°, which results in a modulation spatial frequency of approximately half of the cutoff frequency of the objective. The modulation frequency is selected to optimize the image quality in thick tissue imaging in terms of spatial resolution enhancement and optical sectioning. Other components involved in SIM illumination pattern generation include a half-wave plate (HWP, AHWP05M-600, Thorlabs), an electro-optic modulator (EOM, EO-PM-NR-C4, Thorlabs), and a liquid crystal retarder (LCR, LCC1411-A,

Thorlabs). As a polarization-dependent phase modulator, the EOM is responsible for shifting the phase of one of the half beams relative to the other one. By applying appropriate driving signals to the EOM, the generated line pattern can be quickly phase-shifted for the proper acquisition of raw SIM images. Typically, the phase switching frequency of the EOM is identical to the image acquisition rate of the raw images. The HWP and LCR are polarization manipulation devices for maximizing the modulation depth. The HWP changes the beam to a 45° polarization orientation to make sure the beam power can be separated equivalently by the Wollaston prism. The LCR is used to adjust the polarization orientation of one of the output beams from the Wollaston prism so that they can interfer and generate illumination patterns with optimal modulation depths. As the excitation is condensed to a thin line, a large beam, one-dimensional galvo mirror GM1 (GSV011, Thorlabs), is used to rapidly scan the excitation line pattern along the orthogonal direction for two-dimensional imaging. The typical scanning speed of the galvo mirror is 10 to 100 Hz according to the image frame rate.

The fluorescence emissions from the sample are collected by the same objective lens and de-scanned by GM1. An adjustable slit (VA100; Thorlabs) is placed at the confocal position, which is conjugated to the illumination line focus, to reject the out-of-focus light. Most backscattered excitation light is adequately attenuated by the combination of a dichroic mirror (Green/Orange-DM; Optolong) and emission filters (FITC-EM/TRITC-EM; Optolong). Fluorescence photons are captured using a scientific CMOS camera (OptiMOS^{TM}, Qimaging), which features a sensor size of 1920 x 1080 pixels and a full-frame rate of up to 100 fps. Another galvo mirror GM2 is operated in synchronization with GM1 to rescan the photons emitted from the scanning line focus across the image sensor. The rescan ratio can be adjusted by driving the two galvo mirrors with electrical signals of differential amplitudes.

A multifunction data acquisition card (PCIe-6251, National Instruments) and a Virtual Instrument Software Architecture port are used to deliver control/driving signals and synchronize the sCMOS camera, galvo mirror scanners, and the EOM.

NOTE S4. Sample preparation

Preparation of fluorescent beads phantoms

To characterize the imaging performance of our imaging system, Fluoresbrite® Yellow Green Microspheres from Polysciences were used, which have an excitation maximum at 441 nm and an emission maximum at 486 nm. For quantifying the super-resolution enhancement, we prepared a thin layer of gel mixed with 1 μL 100 nm fluorescent beads (Catalogue No. 17150) and 1mL 2% agarose solution. Agarose was used to immobilize the beads and also provided a transparent and non-scattering background during imaging. The beads mixture was then vortexed on a vortex mixer, poured into a center well dish (MatTek, P35G-0-10-C), and allowed to stand until solidification for imaging.

For demonstrating imaging performance in thick scattering media, a thick bead phantom was prepared to mimic the scattering properties of biological tissues. In order to increase the signal level in deep regions, large beads (2 μm in diameter) were used in the scattering medium. Because beads with large diameters can allow more surface area for fluorophore to be excited and thus generate more fluorescence photons at the same excitation power[19]. We uniformly dispersed 10 μL 2 μm fluorescent beads aqueous suspension (Catalog No. 18140-2) in 40 μL 20% Lipofundin MCT/LCT emulsion (B.Braun Melsungen AG, Germany). Then 350 μL of melted agarose solution was added to the above solution. The total 400 μL solution was pipetted into the well of a single concavity glass microscope slide(1.2 - 1.3 mm thick) and then sealed with a coverslip using nail polish. The beads phantom thus had a concentration of 2% lipid emulsion and a density of 1137 fluorescent beads per μL. According to the calculation using the Mie theory calculator, the isotropic scattering factor g is about 0.715, and the scattering

coefficient μ_s is about 113.3 cm^{-1}, which gives a reduced scattering coefficient of $\mu_s' = (1-g)\mu_s = 32.3cm^{-1}$. This value is close to the average reduced scattering coefficient of biological tissues[20].

Preparation of HeLa cell sample

To prepare the live HeLa cell fluorescence slide, we labeled the F-actin of the HeLa cells using Texas Red™-X Phalloidin (Invitrogen). Firstly, HeLa cells (ATCC) were cultured in high-glucose Dulbecco's modified Eagle's medium (DMEM) supplemented with 10% fetal bovine serum (FBS), 100 units/mg of penicillin, and 100 μg/mL of streptomycin at 37 °C and 5% CO2. For labeling with Texas Red™-X Phalloidin, Hela cells were seeded on coverslips in 24-well plates at the density of 7×10^4 cells per well in a 0.5 ml growth medium and allowed to grow for 20~24 h. Next, the cells were washed with 1x PBS three times, followed by fixation with 4% paraformaldehyde and permeabilization with 0.1% Triton X-100. The cells were then stained with phalloidin solution (0.165 mM) for 30 min and washed with PBS. Finally, the coverslip with fixed cells was mounted onto a glass slide with FluoshieldTM (Sigma) and ready for imaging.

Preparation of mouse brain section

To prepare the mouse brain slice, the Thy1-EGFP transgenic mouse brain was fixed in 4% paraformaldehyde in PBS (w/v) overnight at 4 °C. 250-μm vibratome sections were generated by sectioning tissues embedded in 2% agarose with a vibrating microtome (Leica) and permeabilized in 2% TritonX-100 in PBS (v/v) overnight at 4 °C. RapiClear 1.52 (SunJin Lab Co), which is a water-soluble clearing reagent for enhanced visualization of biological specimens, was used to clear sections according to the manufacturer's instructions. After 1 hour, the mouse brain slice became transparent and was mounted in an iSpacer microchamber(SunJin Lab Co). The space outside the microchamber was filled with nail polish to ensure a safety seal.